Accuracy of solitary wave generation by a piston wave maker

Katell Guizien, Eric Barthélemy

Accuracy of solitary wave generation by a piston wave maker.

Précision de la génération d'une onde solitaire par un batteur piston.

GUIZIEN KATELL, *Laboratoire des Ecoulements Géophysiques et Industriels, BP 53, 38041 Grenoble Cedex 9, France. Tél: +33 4 76 82 51 17 / Fax: +33 4 76 82 50 01 / E-mail: guizien@hmg.inpg.fr*

BARTHÉLEMY ERIC, *Laboratoire des Ecoulements Géophysiques et Industriels, BP 53, 38041 Grenoble Cedex 9, France.*

ABSTRACT

A new experimental procedure to generate solitary waves in a flume using a piston type wave maker is derived from Rayleigh's (1876, [18]) solitary wave solution. Resulting solitary waves for dimensionless amplitudes ε ranging from 0.05 to 0.5 are as pure as the ones generated using Goring's (1978, [7]) procedure which is based on Boussinesq (1871a, [1]) solitary wave, with trailing waves of amplitude lower than 3 % of the main pulse amplitude. In contrast with Goring's procedure, the new procedure results in very little loss of amplitude in the initial stage of the propagation of the solitary waves. We show that solitary waves generated using this new procedure are more rapidly established. This is attributed to the better description of the outskirts decay coefficient in a solitary wave given by Rayleigh's solution rather than by a Boussinesq expression. Two other generation procedures based on first-order (KdV) and second order shallow water theories are also tested. Solitary waves generated by the latter are of much lower quality than those generated with Rayleigh or Boussinesq-based procedures.

RÉSUMÉ

Une nouvelle procédure expérimentale pour générer des ondes solitaires dans un canal à l'aide d'un batteur piston est proposée à partir de la solution onde solitaire de Rayleigh (1876, [18]). Les ondes solitaires produites pour des amplitudes réduites ε allant de 0.05 à 0.5 sont aussi pures que celles obtenues par Goring (1978, [7]) à l'aide d'une procédure basée sur l'expression onde solitaire de Boussinesq (1871a, [1]). L'amplitude des ondes suivant le pic principal ne dépasse pas 3 % de l'amplitude de celui-ci. Le pic principal des ondes générées avec cette nouvelle procédure diminue très peu en amplitude, contrairement à celles de Goring. On montre que les ondes générées à l'aide de cette procédure sont donc plus rapidement établies. Ceci est attribué à une meilleure description du paramètre de tendance dans la solution onde solitaire de Rayleigh que dans l'expression de Boussinesq. Deux autres procédures basée sur les théories au premier et second ordre de l'eau peu profonde sont aussi testées. Les ondes solitaires générées par ces deux dernières procédures sont de bien moindre qualité que celles obtenues avec les procédures basées sur Rayleigh ou Boussinesq.

Keywords : solitary wave, generation, piston wave maker, experiments.

1. Introduction

The aim of this study is to assess solitary wave generation procedures. Hammack and Segur (1974, [10]) showed experimentally and theoretically that from any net positive volume of water above the still water level, at least one solitary wave will emerge followed by a train of (dispersive) waves. Thus, different procedures have been used to generate solitary waves. Scott Russel (1845, [20]) generated solitary waves by allowing a solid weight to fall from near the surface to the bottom of a tank. Similarly, Daily and Stephan (1952, [6]) displaced a given mass of water by the vertical motion of a piston rising from the bottom of a tank. They also tested a method consisting in releasing a mass of water behind a moveable barrier at one end of a flume. Goring (1978, [7]) studied in detail the generation of solitary waves using a piston-type wave maker.

Our concern in this study is to generate solitary wave as 'pure' as possible. This means we have focussed our efforts in generating waves with minimised trailing waves but also of stable amplitude during propagation. These concerns have scientific practical importance. For instance, the study of solitary wave reflection (Renouard et al., 1985 [19]) or of interaction of either solitary waves with solitary waves or monochromatic waves with solitary waves (Guizien and Barthélemy, 2000 [9]) require waves as pure as possible, especially if phase shifts are to be measured.

Since long waves are associated to quasi vertically uniform horizontal velocity, the piston-type wave maker seems a natural generation device. However it is technically more difficult to set up than the other generation means cited above. Without paying much attention to the way in which the generator is displaced (mass falling or rising, barrier, wave maker), the success of all these methods is based on the fact that the largest solitary wave outruns any transient dispersive disturbance and also any other solitary wave of lower amplitude for sufficient propagation distances. Indeed, as the dimensionless amplitude of a solitary wave increases up to $\varepsilon = 0.796$ ($\varepsilon = A/h_0$ where A is the solitary wave amplitude and h_0 is the mean water depth), its phase speed increases. However, above this value, the phase speed tends to decrease (Longuet-Higgins and Fenton, 1974 [15], Byatt-Smith and Longuet-Higgins, 1976 [4]). Regarding generation, this feature raises a major problem, as highlighted by Longuet-Higgins (1981, [14]) because, together with the phase speed, the total displaced mass decreases over the upper range of solitary wave amplitude. Hence, there are actually two waves of different amplitude with the same displaced mass. Thus, using the aforementioned procedures, two distinct solitary waves may emerge. However, in most applications, generating the largest solitary wave is not so important.

The usual procedure for long-wave and more specifically solitary-wave generation consists in matching the paddle velocity at each position in time with the vertically averaged horizontal velocity of the wave. Mathematically this is expressed in the following way:

$$\frac{dX}{dt} = \bar{u}(X,t) \tag{1}$$

where $x = X$ is the paddle position along the x–axis and $\bar{u}(x,t)$ is the long wave depth-averaged horizontal velocity in the laboratory frame of reference. The x–axis is the centreline of the flume, taking the origin $x = 0$ at the back position of the piston stroke as defined on figure 1. This contrasts with the approach taken by Synolakis (1990, [23]) who solved an inverse evolution problem of the Korteweg-De Vries (KdV) equation in order to generate arbitrary long waves at any location in a horizontal flume.

In the present paper, we discuss Goring's procedure which is based on Boussinesq (1871a, [1]) solitary wave solution in comparison with four generation laws derived from other existing solitary wave solutions. Two generation laws are obtained using Rayleigh's (1876, [18]) solitary wave solution. Indeed, by assuming a small displacement, an analytical law of motion can be derived from the integration of equation (1) in which the Rayleigh solitary wave solution is used. This analytical law of motion is compared with a law of motion obtained after fitting the numerical integration of equation (1), also using Rayleigh's solution, by a hyperbolic tangent. The other two laws of motion tested in this study are derived from linearization of the Lagrangian formulation in the first-order (or Korteweg and De Vries) and second-order shallow water theories (Temperville, 1985 [24]). In our experiments, we use a very similar device to the one used by Goring, that is described in section 3. In section 4, performances of the tested laws of motion are compared. In order to understand the good performance of both Goring procedure and the law of motion based on Rayleigh's solitary wave solution, paddle laws of motion are discussed in section 5 in comparison with the one deduced from Byatt-Smith's (1970, [3]) numerical solution.

2. Wave maker laws of motion

In this section, we present the different laws of motion to be prescribed to the paddle in order to generate a solitary wave. A solitary wave is a steady solution in the wave co-moving frame travelling at the wave phase speed c. Hence, equation (1), that gives the paddle position X in the laboratory frame of reference, can be written after a change of variables from (x,t) to $(\theta = ct - X, t)$ in the general form:

$$\frac{dX}{d\theta} = \frac{\bar{u}(\theta(X))}{c - \bar{u}(\theta(X))} \tag{2}$$

In equation (2), the solitary wave depth-averaged horizontal velocity can be given by various theories. Amongst them, the Boussinesq (1871a, [1]) and Rayleigh (1876, [18]) solitary waves have the following same functional form:

$$\eta(\theta) = A\,\mathrm{sech}^2(\beta\theta/2) \tag{3}$$

$$\bar{u}(\theta) = \frac{c\eta(\theta)}{h_0 + \eta(\theta)} \tag{4}$$

where A is the solitary wave amplitude, h_0 the mean water depth, c the phase speed, β the outskirts decay coefficient, $\eta(\theta)$ the free surface elevation from rest and $\bar{u}(\theta)$ the depth-averaged horizontal velocity. The two solitary wave expressions differ in terms of the values of c and β. Then, integrating (2) with (3) and (4) yields:

$$X(t) = \frac{2A}{h_0\beta}\tanh[\beta(ct - X(t))/2] \tag{5}$$

From (5), the total stroke of the paddle S can be deduced:

$$S = \frac{4A}{h_0\beta} \tag{6}$$

The duration τ of the paddle motion can be determined after truncation of the infinite theoretical law of motion:

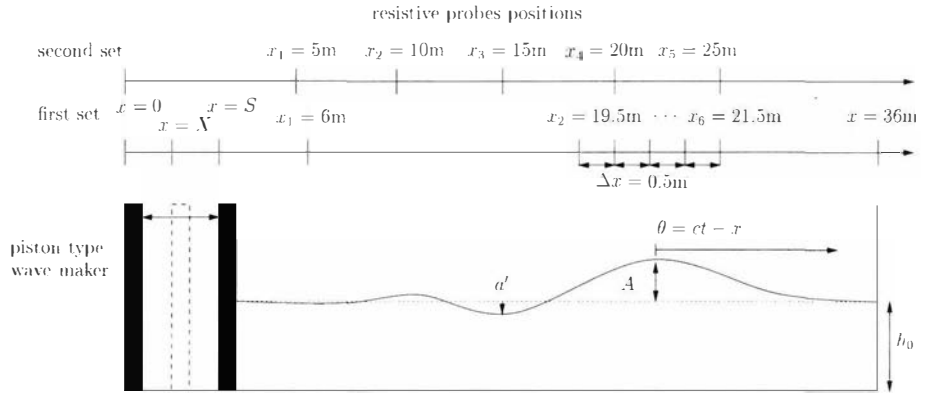

Fig. 1 Sketch and dimensions of the experimental equipment. The x_i's are the resistive probes positions. ($0.2 \le h_0 \le 0.3$ m, $0.015 \le A \le 0.15$ m, $a' \le 0.1\,A$, $S \le 0.55$ m).

$$\tau = \frac{4}{\beta c}\left(\tanh^{-1}(0.999) + \frac{A}{h_0} \right) \tag{7}$$

2.1 Goring/ Boussinesq

In his study, Goring (1978, [7]) first tackled the question of minimising trailing waves in solitary waves generation. He chose a procedure based on the Boussinesq (1871a, [1]) solitary wave expression. Following Daily and Stephan's (1952, [6]) conclusions regarding the best agreement of this expression with experiments, he chose the following values for c and β in (5):

$$\frac{\beta_B}{2} = \sqrt{\frac{3A}{4h_0^3}} \tag{8}$$

$$c_B = \sqrt{g(h_0 + A)} \tag{9}$$

In his study, Goring used both a paddle law of motion derived from the full equation (5) and a simplified paddle law of motion taking $\bar{u}(X,t)$ to be equal to $\bar{u}(0,t)$ in equation (1). This yields the following expression:

$$X(t) = S_G \tanh[7.6(t/\tau - 0.5)]$$

where $S_G = 4\sqrt{\frac{Ah_0}{3}}$ is the total stroke of the paddle.

These two laws of motion were prescribed for the paddle by means of a hydraulic servo-system. The solitary waves generated experimentally using the simplified procedure were followed by a dispersive tail of 10 % of the amplitude of the main pulse. Using the paddle law of motion derived from the full equation, trailing wave amplitude is drastically reduced. Yet, it was noted that by taking a duration of motion 10 % longer than that given by (7) with (8) and (9), the amplitude of the trailing dispersive waves was even more reduced. The two experimental records plotted by Goring ([7], pp 123 and 130) show nearly pure solitary waves generated using this longer duration. Yet, the resulting solitary waves show a rapid decrease in amplitude, larger than what can be attributed to friction.

2.2 Shallow water first order/KdV

Clamond and Germain (1999, [5]) used a paddle law of motion $X_{KdV}(t)$ derived from the KdV (or first-order shallow water) solution and written:

$$X_{KdV}(t) = 2\sqrt{\frac{Ah_0}{3}} \tanh(\beta_{KdV} c_{KdV} t/2) \tag{10}$$

where $\beta_{KdV} = \sqrt{\frac{3A}{h_0^3}}$ and $c_{KdV} = \sqrt{gh_0}\left(1 + \frac{A}{2h_0}\right)$. The paddle stroke is thus $S_{KdV} = 4\sqrt{\frac{Ah_0}{3}}$, the same as that derived from Boussinesq's solitary wave form in Goring's procedure. This is obtained from calculations in Lagrangian form after linearization around $X = 0$.

2.3 Shallow water second order

In the same way and following calculations from Temperville (1985, [24]), a second-order shallow-water paddle law of motion can be derived. For a solitary wave of amplitude A, the paddle law of motion $X_{SW2}(t)$ is:

$$X_{SW2}(t) = 2\sqrt{\frac{A'h_0}{3}}\left(1 + \frac{A'}{h_0}\right)\tanh(\beta_{SW2} c_{SW2} t/2) + \frac{A'}{3}\sqrt{\frac{3A'}{4h_0}}\frac{\tanh(\beta_{SW2} c_{SW2} t/2)}{\cosh^2(\beta_{SW2} c_{SW2} t/2)} \tag{11}$$

where $\beta_{SW2} = \sqrt{\frac{3A'}{h_0^3}}$, $c_{SW2} = \sqrt{gh_0}\left(1 + \frac{A'}{2h_0} + \frac{19}{40}\left(\frac{A'}{h_0}\right)^2\right)$ and $\frac{A}{h_0} = \frac{A'}{h_0}\left(1 + \frac{5A'}{4h_0}\right)$.

The paddle stroke is thus $S_{SW2} = 4\sqrt{\frac{A'h_0}{3}}\left(1 + \frac{A'}{h_0}\right)$. In practice this law is truncated with respect to the precision of experimental device and the last term can be neglected.

2.4 Rayleigh

Shallow water approximation relies on both long waves and small amplitude assumptions. Avoiding the latter restriction of small amplitude, it is possible to derive a set of equations for non linear waves (Mei, 1992 [16]). Indeed, assuming the Ursell number $U_r = \varepsilon/\sigma^2$ to be of order 1 ($\varepsilon \approx \sigma^2$ with $\sigma = h_0/\lambda$ where $\lambda = 2/\beta$ is a horizontal length scale of the solitary wave), Whitham (1974, [25]) derived the Boussinesq equations (see eq. (13.101) in Whitham, 1974 [25]). Without making this assumption, namely allowing ε to be of order 1, the following set of equations is derived after truncating at the order σ^4 (Serre, 1953 [21], Su and Gardner, 1969 [22]):

$$\eta_t + \left[(h_0 + \eta)\bar{u}\right]_x = 0 \tag{12}$$

$$\bar{u}_t + \bar{u}\bar{u}_x + g\eta_x - \frac{2}{3}\gamma\eta_x + \frac{h_0 + \eta}{3}\gamma_x = 0 \tag{13}$$

$$\gamma = (h_0 + \eta)\left(\bar{u}_x^2 - \bar{u}\bar{u}_{xx} - \bar{u}_{xt}\right) \tag{14}$$

Serre (1953, [21]) found a solitary wave solution for this set of equations which is actually the solitary wave solution that Rayleigh (1876, [18], see also Lamb, 1932 [13]) found for the steady progressive solution described by Russel and has the form (3) taking:

$$\frac{\beta_R}{2} = \sqrt{\frac{3A}{4h_0^2(A + h_0)}} \tag{15}$$

$$c_R = \sqrt{g(A + h_0)} \tag{16}$$

It should be noted here that Rayleigh's solitary wave solution differs from the conjectured Boussinesq solitary wave form by the

outskirts decay coefficient β (Miles, 1980 [17]). The paddle position X is thus given by equation (5) incorporating (15) and (16).

Hence, the paddle stroke is given by $S_R = 4\sqrt{\frac{A(A+h_0)}{3}}$.

Equation (5) together with (15) and (16) can be solved either numerically or, if small displacements are assumed, explicitly after linearization:

$$X_R(t) = \frac{2A}{h_0\beta_R}\frac{h_0\tanh(\beta_R c_R t/2)}{h_0 + A\left[1-\tanh^2(\beta_R c_R t/2)\right]} \qquad (17)$$

A hyperbolic tangent function of the form $X(t) = \alpha\tanh(\delta t)$ can be fitted in the least square sense on the numerical integration of equation (5), where c and β are given by (15) and (16). The coefficients α and β corresponding to the experiments are reported in table 1.

Table 1 Coefficients for the hyperbolic tangent function $\alpha\tanh(\beta t)$ fitted on the numerical integration of (1) for Rayleigh's solitary wave solution.

ε	h_0 = 0.2 m		h_0 = 0.3 m	
	α	β	α	β
0.05	-	-	0.0795	1.0622
0.10	0.0768	1.7675	0.1152	1.4432
0.15	-	-	0.1446	1.7000
0.20	0.1139	2.3147	0.1708	1.8899
0.25	-	-	0.1952	2.0364
0.30	0.1457	2.6349	0.2185	2.1513
0.35	-	-	0.2409	2.2427
0.40	0.1752	2.8356	0.2628	2.3152
0.45	-	-	0.2843	2.3726
0.50	0.2036	2.9607	-	-
0.60	0.2314	3.0337	-	-

For practical purposes, the paddle laws of motion are all truncated using the following same criterion, namely by imposing $\tanh(\delta t) = 0.9999$. Figure 2 shows these different laws of motion for the same expected resulting solitary wave. The two paddle laws of motion derived from Rayleigh's solution lead to larger paddle displacements than paddle laws of motion derived from KdV or second-order shallow-water theory. As paddle displacements are limited by jack length, the maximum dimensionless amplitude generated using paddle laws of motion derived from Rayleigh's solution would be smaller than those derived from KdV.

3. Experiments description

The experiments are conducted in a 36 m long, 0.55 m wide and 1.2 m high flume as sketched on figure 1. At one end of the flume a piston-type wave maker can be displaced horizontally. The piston is linked to a hydraulic jack capable of a 550 mm stroke. The control system is monitored by a computer. Different motions of the paddle can be prescribed by the computer, enabling the generation of either solitary waves or sinusoidal waves. Nevertheless the piston-type wave maker is more appropriate for long wave generation since it displaces the entire water column uniformly. However, we need to prescribe the appropriate law of motion for the paddle in order to produce solitary waves that are as pure as possible. The different laws of motion detailed in the previous sections are tested. A solitary wave of expected amplitude A is generated using each law. The two Rayleigh laws require larger paddle displacement than the shallow-water laws. With regard to the finite stroke of the jack, the laws deduced from the Rayleigh solution lead to smaller solitary wave amplitudes.

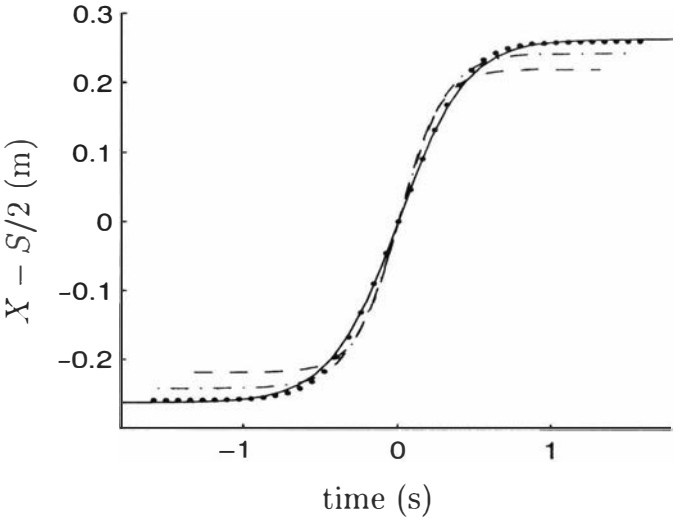

Fig. 2 The four laws of motion tested for a solitary wave of dimensionless amplitude ε = 0.4 with a water depth h_0 = 0.3 m: first-order shallow water (- –); second-order shallow water (-.-); hyperbolic tangent fitted to Rayleigh numerical integration (–); analytical linearization of Rayleigh-based law of motion (...).

For a water depth h_0 = 0.3 m, the upper bound of the solitary wave dimensionless amplitude $\varepsilon = A/h_0$ is 0.35, while using the first-order shallow water law allows a dimensionless amplitude up to 0.5. We generate the broader range of dimensionless solitary wave amplitudes possible for depths at rest of h_0 = 0.3 m (ε varies from 0.05 to 0.35) and h_0 = 0.2 m (ε varies from 0.1 to 0.6). Surface displacements during the experiments are measured in fixed locations by resistive probes. Probe precision is estimated to be 0.5 mm for free surface elevations lower than 5 cm and at 1 mm beyond this limit. This is due to probe calibration (Guizien, 1998 [8]). This means that the relative error in the dimensionless amplitude is about 3 % for the smallest solitary waves (ε = 0.05) and is less than 2 % for the others. All experimental recordings are measurements of free surface displacement against time (between 15 and 25 seconds duration). Two series of experiments were performed. In the first set (h_0 = 0.2 m and h_0 = 0.3 m), the probes are located along the centreline of the flume to avoid lateral perturbations, at x_1 = 6 m and every 0.5 m between x_2 = 19.5 m and x_6 = 21.5 m. In the second set (h_0 = 0.3 m), five probes are located every 5 m up to 25 m. All distances are given from the flume end where the paddle is located.

4. Experimental results

Figures 3 shows the free surface elevation measured at a distance $x = 67\ h_0$ from the wave maker end of the flume, corresponding to solitary waves generated using the four paddle laws of motion with $\varepsilon = a/h_0$ ranging from 0.05 to 0.35 for $h_0 = 0.3$ m. Figures 4 represents the same measured at $x = 100 h_0$ from the paddle with ε ranging from 0.1 to 0.6 for $h_0 = 0.2$ m. These measurements correspond to the first set of experiments.

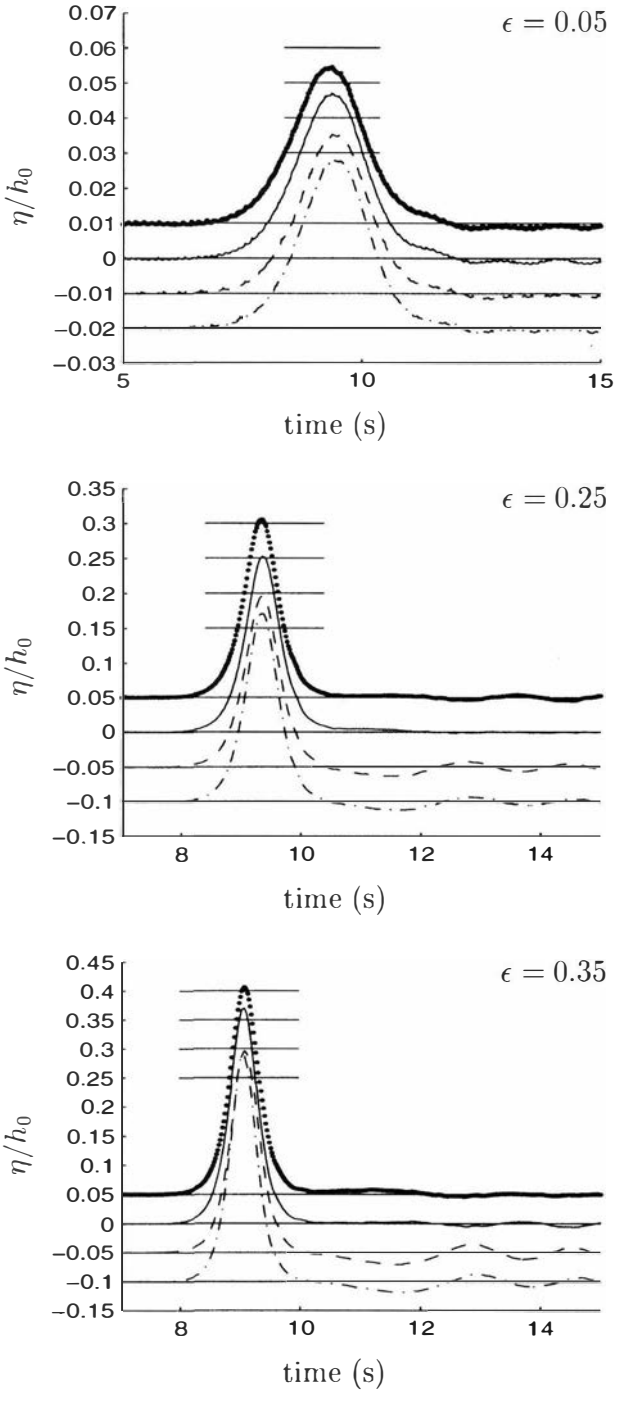

Fig. 3 Solitary waves generated using the 4 laws of motion considered (same legend as fig.1 – The horizontal solid line represents the prescribed main pulse amplitude.) – Record of free surface elevation at $x = 67\ h_0$ away from the paddle with $h_0 = 0.3$ m.

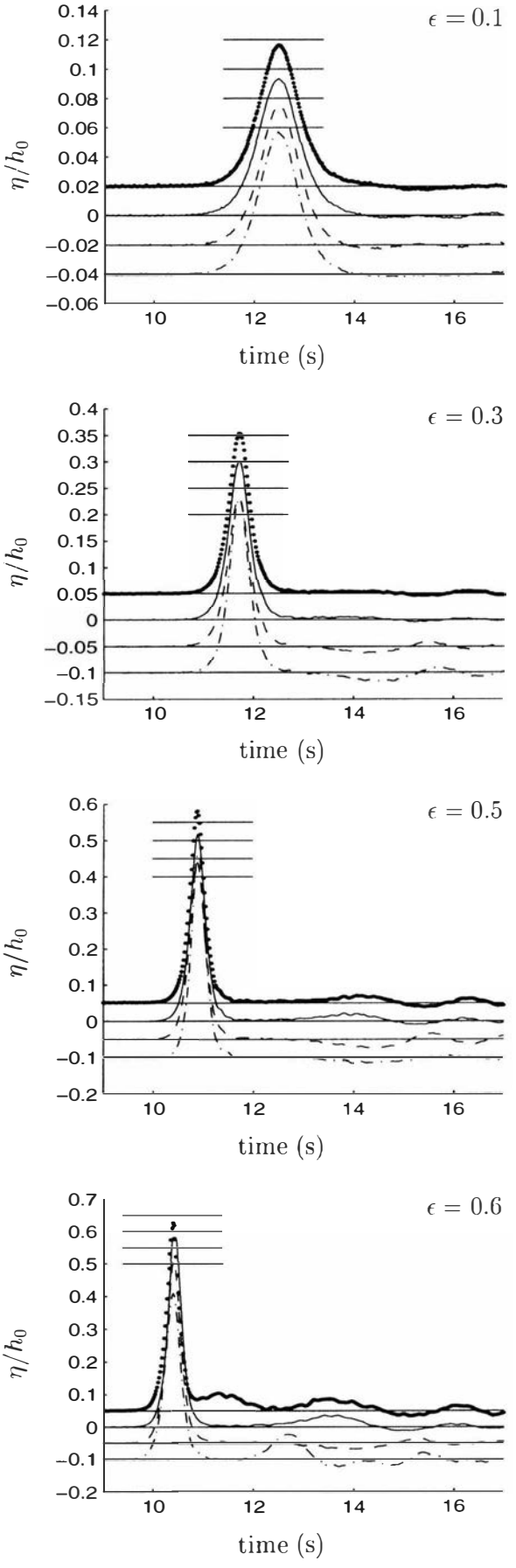

Fig. 4 Solitary waves generated using the 4 laws of motion considered (same legend as fig. 1 and 3) – Record of free surface elevation at $x = 100\ h_0$ away from the paddle with $h_0 = 0.2$ m.

All solitary waves generated using a paddle law of motion derived from KdV or second-order shallow water theory exhibit a trough (dispersive wave) after the main pulse whereas using paddle laws of motion derived from Rayleigh, a bump (maybe a smaller solitary wave) trails it. It is noticeable that the bumps are of smaller amplitude than the troughs, except for the largest waves with $\varepsilon = 0.6$ for $h_0 = 0.2$ m. Indeed, this case behaves differently. There is sometimes breaking or two solitary waves are clearly generated for laws of motion giving good results for lower amplitudes and the worst law of motion suddenly gives better results. This latter feature was already observed for $\varepsilon = 0.5$ with the second-order shallow water procedure. In fact, the limit of the dynamic servo-controller is reached for such waves. The discrepancy between the prescribed and actual paddle motion is no longer negligible, due to the very large acceleration required. On figure 5, the paddle laws of motion corresponding to the hyperbolic tangent function fitted to a Rayleigh numerical integration are plotted for ε ranging from 0.1 to 0.6. Greatest accelerations occur somewhere between the beginning of motion (zero velocity) and mid-stroke (maximum velocity). Qualitatively, the larger the maximum velocity and the shorter the duration of motion, the greater the acceleration. From figure 5, it may be expected that the maximum acceleration will increase with the amplitude of the solitary wave and may reach the limit of the servo-controller. From figure 2, it may also be noted that for a prescribed amplitude, the law of motion based on the second-order shallow water theory requires greater acceleration than the other procedures. This explains why for this law of motion the servo-controller limit is already reached when $\varepsilon = 0.5$. Thus, we will exclude from our discussion the $\varepsilon = 0.6$ experiment for all laws and the $\varepsilon = 0.5$ experiment for the second-order shallow water theory based procedure. Indeed, except for these cases, the actual paddle law of motion is sufficiently close to the prescribed one.

4.1 Trailing waves

Confident in the assumption that the system is capable of following the desired law of motion, our interest is to minimise the trailing waves. On fig. 6.a and .b, we present the amplitude a' of these bumps or troughs with respect to the main pulse amplitude measured at $x = 67h_0$ (resp. $x = 100h_0$) away from the paddle end of the flume for $h_0 = 0.3$ m (resp. $h_0 = 0.2$ m). The trough amplitudes (on average 5 %) are sometimes more than twice those of the bumps (on average 3 %). We also discuss the four procedures tested in our experiments in comparison to Goring's (1978, [7]). The only records plotted in Goring's thesis correspond to small amplitude solitary waves ($\varepsilon = 0.1$, [7], p 123 and $\varepsilon = 0.2$, [7], p 130). In our experiments' equivalent, solitary waves generated using laws of motion derived from Rayleigh's solution show similarly small bumpy trailing waves with less than 3 % amplitude. Measurements of the free surface elevation at different distances from the paddle for a solitary wave of prescribed dimensionless amplitude $\varepsilon = 0.2$ generated using Rayleigh's numerical integration are plotted on figure 7. This graph is comparable to the one produced by Goring ([7], p 130) regarding the trailing waves. Yet, in Goring's experiments, the solitary wave amplitude is severely damped to $\varepsilon = 0.15$ at $x = 85h_0$.

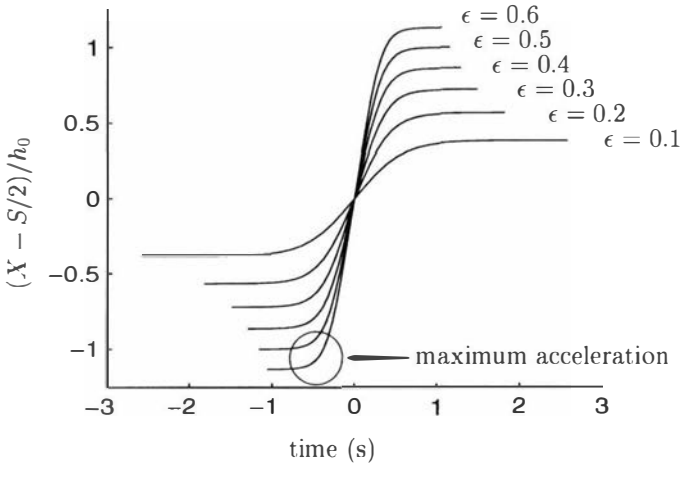

Fig. 5 Laws of motion for solitary waves of dimensionless amplitude ε ranging from 0.1 to 0.6 (h_0 = 0.2 m) obtained from the linearized solution of (5) for a Rayleigh solitary wave. Maximum velocity is reached when $t = 0$ and maximum acceleration occurs where the curvature is the greatest.

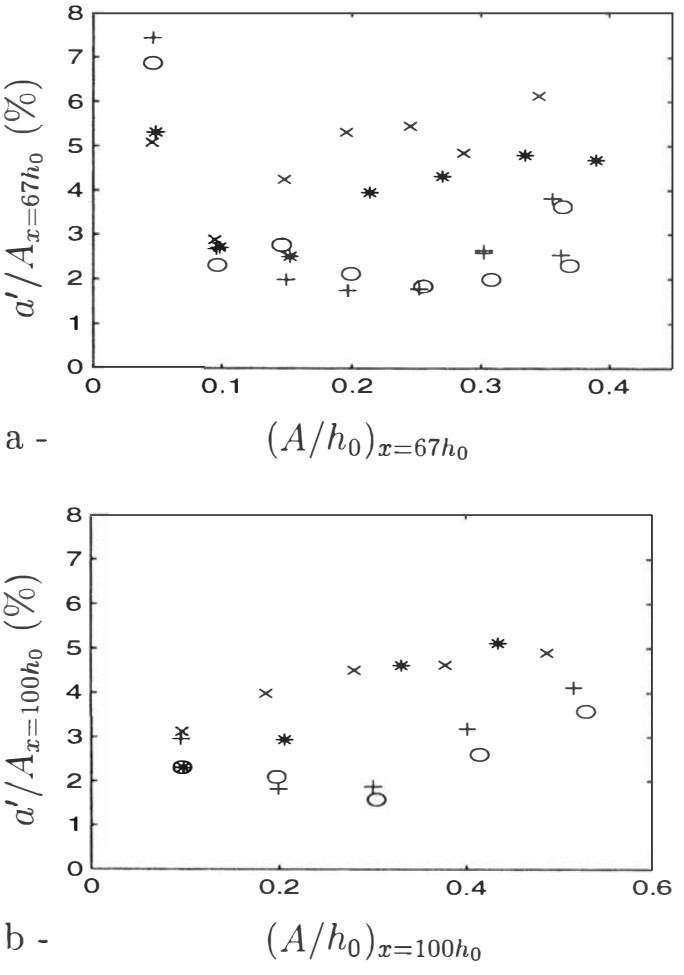

Fig. 6 Relative amplitude of the first trailing wave a' (bump or trough) versus the dimensionless solitary wave amplitude. Solitary waves are generated using paddle laws of motion derived from KdV (x), second-order shallow-water theory (*), Rayleigh analytical (o) and Rayleigh numerical (+) solutions at (a) at $x = 67$ h_0 away from the piston paddle for $h_0 = 0.3$ m and (b) at $x = 100$ h_0 away from the piston paddle for $h_0 = 0.2$ m.

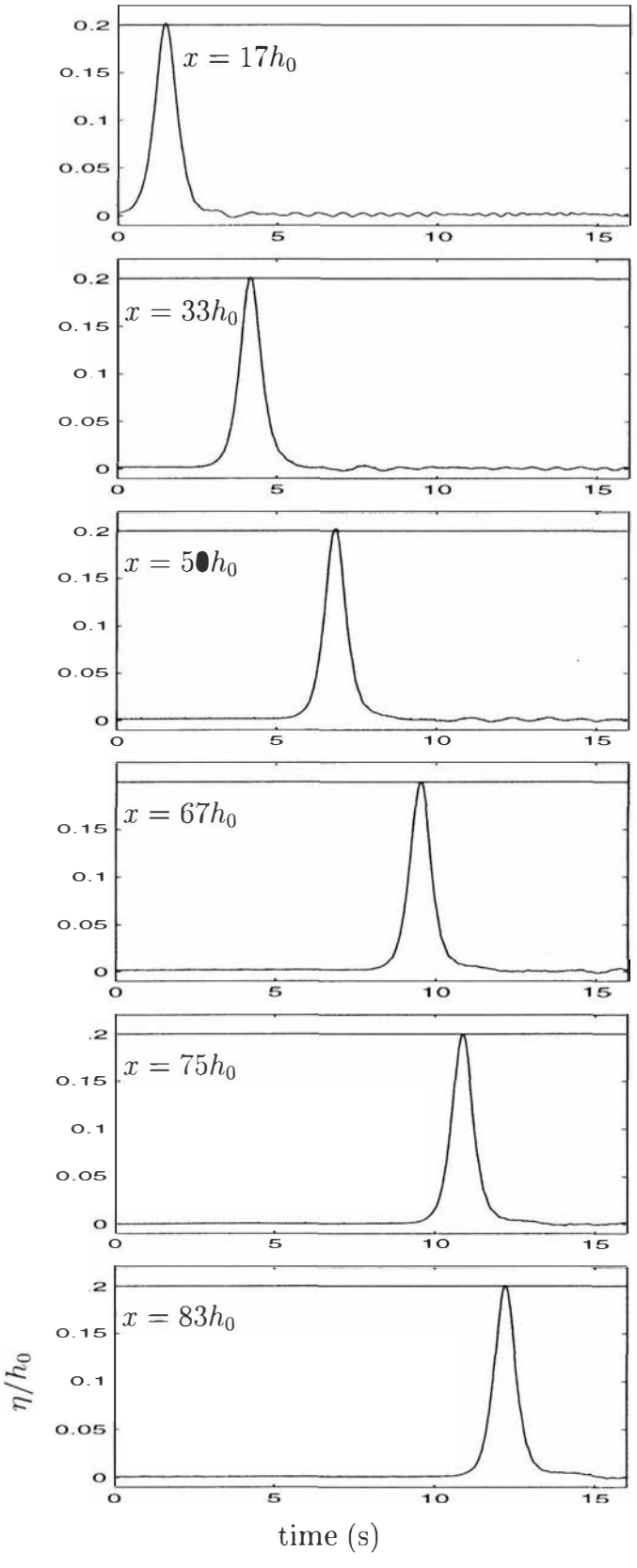

Fig. 7 Solitary waves generated using the paddle motion based on the tanh fit on the numerical integration of equation (2) for Rayleigh solitary wave solution – Record of free surface elevation at different distances from the paddle ($\varepsilon = 0.2$, $h_0 = 0.3$ m).

4.2 Main pulse stability

By reproducing the same generation sequence several times, it becomes clear that the generated wave is highly reproducible, so that for a given paddle law, the solitary wave amplitude could be determined at any location in the flume together with the relative size of the trailing waves given the probe accuracy. During the second set of experiments, we studied the changes occurring in the first moments of propagation of the solitary wave emerging from the KdV and Rayleigh solutions, between $x = 17h_0$ and $x = 83h_0$ for $h_0 = 0.3$ m (see figure 8). In the first and second set of experiments, the amplitude of solitary waves generated using KdV or the second-order shallow water theory clearly decreases more as it propagates than it does when using Rayleigh. This cannot be attributed only to damping by viscous friction as estimated by the Keulegan formula (1948, [11]) although this formula gives a very good prediction of this dissipation, as tested by Renouard et al. (1985, [19]). Indeed, from Keulegan's formula, the amplitude decrease due to viscous dissipation over $\Delta x = 45h_0$ would be 3.3 % whereas the measured damping over the same distance for solitary waves generated using KdV or the second-order shallow water theory varies between 5 and 6 %. For a solitary wave generated using Rayleigh, this damping is no more than 3 %, and on average 1.5 %.

This loss of amplitude is also observed in the experiments by Goring ([7], p 130). Indeed, for a solitary wave of initial dimensionless amplitude $\varepsilon = 0.175$ ($h_0 = 0.1$ m, which is already

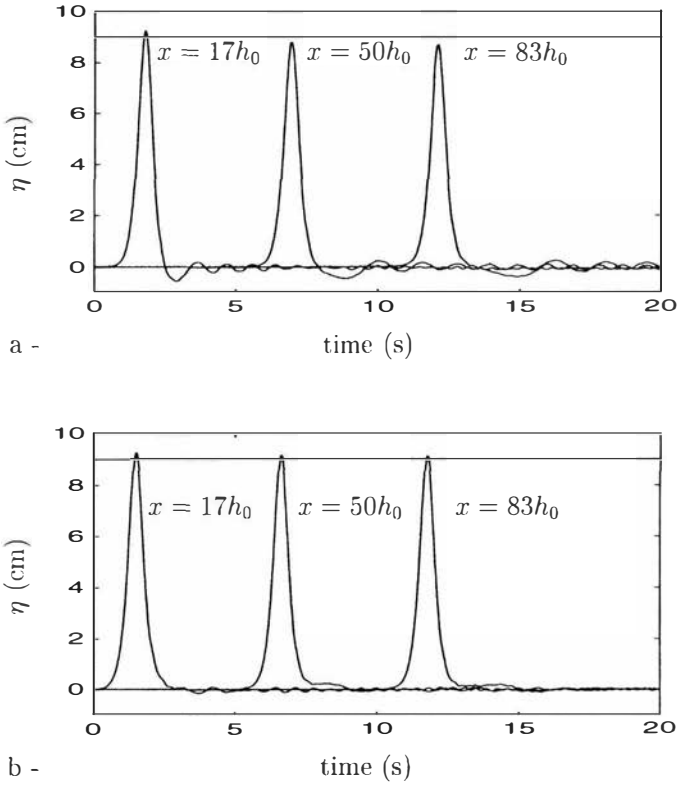

Fig. 8 Solitary waves of dimensionless amplitude $\varepsilon = 0.3$ ($h_0 = 0.3$ m) generated by KdV (a) and Rayleigh (b) based procedures measured at different distances from the paddle. The KdV based procedure results in a solitary wave pulse that decreases. In contrast, the Rayleigh based procedure produces very stable pulses.

lower that the prescribed amplitude $\varepsilon = 0.2$), Goring gives a damping over $\Delta x = 100h_0$ (between $x = 10h_0$ and $x = 110h_0$) of 17 %, whereas the estimation from Keulegan's formula is 11 %. In similar conditions ($\varepsilon = 0.2$, $h_0 = 0.2$ m), our experiments give a damping over $\Delta x = 67.5h_0$ for solitary waves generated using Rayleigh-based procedures of 5.5 % (4.6 % for the tanh fit and 6.2 % for the linearization), and 8 % for shallow water based procedures, while Keulegan's formula predicts a viscous damping of 4.8 %. Figure 9 shows the loss of amplitude for all the sets of experiments performed. These plots contain values given for all the generation laws tested. The trend discussed above appears very clearly. Rayleigh based procedures (and especially the numerical one) result in solitary wave primary pulses whose amplitude decreases less than in the case of those produced by shallow water. Goring noticed that the Boussinesq based procedure produced severely damped solitary waves as well. Moreover the Boussinesq, KdV and second-order shallow water procedures produce trailing waves that need a longer distance to separate from the main pulse. This indicates that energy exchanges between these two parts of the wave train last longer, resulting in less stable primary pulses. For all amplitudes, it is shown that a solitary wave generated using Rayleigh based procedures is stable beyond $x = 20h_0$ while for other procedures the distance can be estimated at $x = 80h_0$. The good performance of laws of motion derived from Rayleigh's solution are probably due to the accuracy with which Rayleigh's solution describes certain characteristics of the exact solitary waves. These aspects are discussed below.

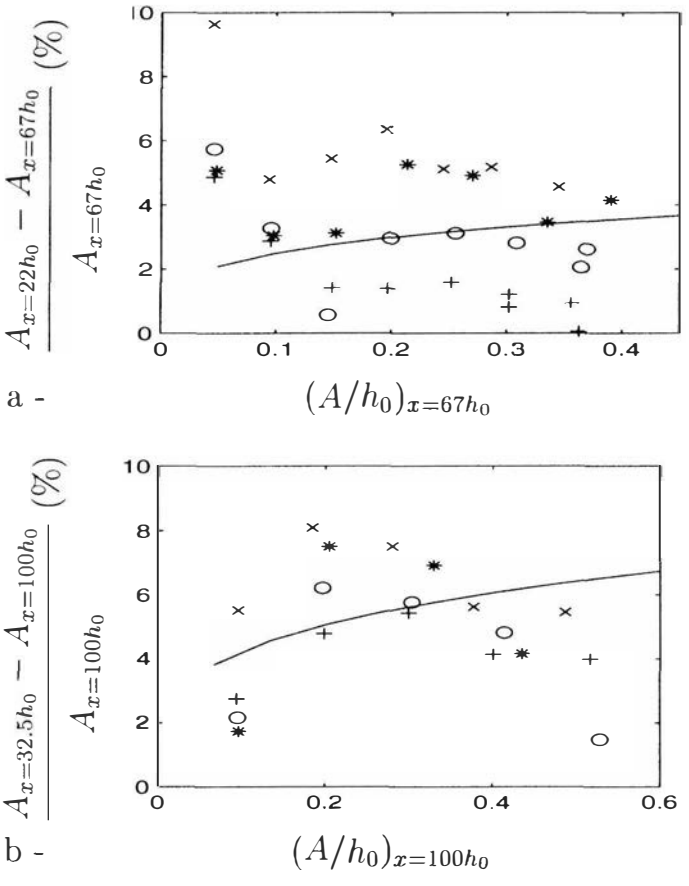

Fig. 9 Loss of amplitude of the main pulse between 6.5 m and 20 m from the paddle versus designed dimensionless amplitudes for solitary waves generated using paddle laws of motion derived from KdV (x), second-order shallow-water theory (*), Rayleigh analytical (o) and Rayleigh numerical (+) solutions for (a) h_0 = 0.3 m and (b) h_0 = 0.2 m. The Keulegan formula estimates are plotted as solid lines.

5. Discussion

The Byatt-Smith (1970, [3]) numerical solution will be used as a reference for the exact solitary wave. It is indeed known to be one of the most accurate solitary wave solution within the potential flow theory. From this solution, the depth-averaged horizontal velocity is easily computed and substituted in (1) to compute a law of motion for the paddle. It should be noted that no experiments were performed using this law. However it is felt that a Byatt-Smith procedure is not very practical since each wave velocity field needs to be computed numerically which is very time-consuming. On figure 10, the dimensionless paddle laws of motion with time for Byatt-Smith, Rayleigh and Boussinesq (Goring procedure) solitary waves and for shallow-water theories are plotted for $\varepsilon = 0.306$. For the same wave we also plot on figure 11 the dimensionless paddle velocity corresponding to these laws of motion. In the example shown on figure 10 it appears that the total paddle stroke is better described by the second-order shallow water solution than by any other solution. Figure 12 plots the depth-averaged net mass displacement L in a solitary wave computed from Byatt-Smith's numerical solution compared to the ones associated to KdV, shallow water second-order and Rayleigh solutions. This net mass displacement is the total stroke of the paddle prescribed in each procedure. Hence, it is confirmed that the total

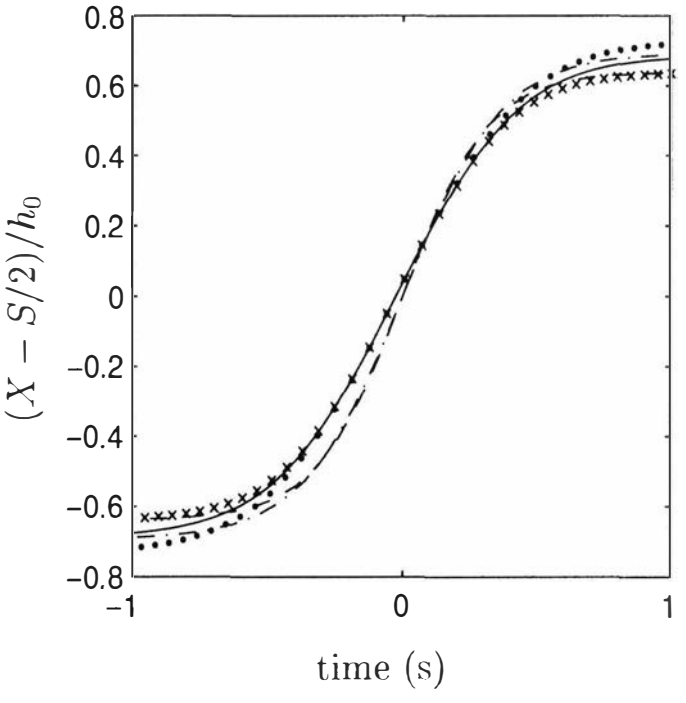

Fig. 10 Paddle law of motion derived from Byatt-Smith's numerical solution (–), KdV solution (- -), second-order shallow water solution (-.-), Rayleigh's solution (...) and Goring's procedure (xxx) for $\varepsilon = 0.306$.

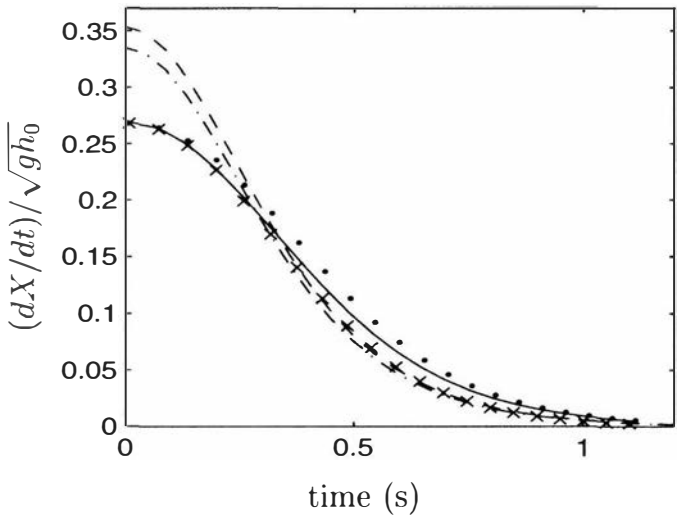

Fig. 11 Dimensionless paddle velocity versus time for Byatt-Smith's numerical solution (–), KdV (- -), second-order shallow water solution (-.-), Rayleigh's solution (...) and Goring's procedure (xxx) for $\varepsilon = 0.306$.

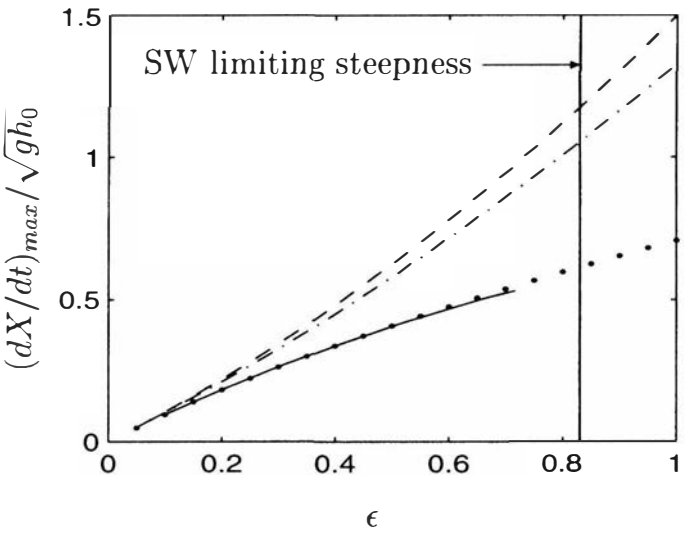

Fig. 13 Dimensionless maximum paddle velocity at mid-stroke for Byatt-Smith's numerical solution (–), KdV (- -), second-order shallow water solution (-.-), Rayleigh's solution (...) versus dimensionless solitary wave amplitude ε.The maximum paddle velocity in Goring's procedure is the same as in the Rayleigh-based procedure.

stroke in the second-order shallow-water theory procedure is the closest to the Byatt-Smith solution mean net mass displacement, at least in the solitary wave dimensionless amplitude range considered in the experiments. Nevertheless, it seems that this good agreement is not sufficient to produce 'pure' solitary waves. Indeed, trailing waves are smaller when using Goring or Rayleigh procedures and yet, total strokes are smaller and larger respectively in Goring and Rayleigh procedures compared to the Byatt-Smith mean net displacement. Figure 11 also shows that the Boussinesq and Rayleigh paddle velocities closely match the velocity required by Byatt-Smith's solution. In fact, in both procedures, paddle laws of motion match the Byatt-Smith based paddle motion around mid-stroke (fig. 10), where the paddle velocity reaches its maximum (fig. 11). Indeed, the maximum paddle velocity deduced from Byatt-Smith solution (which occurs at mid-stroke) is very well described by the Rayleigh or Boussinesq solutions (there are equals) over a broad range of dimensionless amplitudes as shown on figure 13. As shown by (4) a good estimation of the maximum depth-averaged velocity requires a good estimation of the phase speed. The dimensionless phase speed (or Froude number) $F = c/\sqrt{gh_0}$ is plotted on 14.a. It shows that the Rayleigh phase speed is the closest to both the Byatt-Smith numerical and experimental estimations. The outskirts decay coefficient versus the dimensionless amplitude is plotted on figure 14.b. This outskirts decay coefficient describes the way free surface elevation tends towards the mean level at infinity. Stokes showed that β is a solution of the following equation, also used by Byatt-Smith:

$$F^2 = \frac{\tan(\beta)}{\beta} \qquad (18)$$

It should be underlined here that the Boussinesq solitary wave expression is neither a solution of the KdV nor of the Boussinesq equations (1872, [2]). It appears to be a mixture of the Rayleigh phase speed and of the KdV outskirts decay coefficient and consequently, net mass transport. Concerning the outskirts decay coefficient, the same hierarchy as for the phase speed is observed on figure 14.b. This explains why the paddle velocity in Rayleigh's procedure matches the paddle velocity based on Byatt-Smith solution both at the maximum and the outskirts.

As a matter of fact none of these approximate solutions matches the Byatt-Smith reference with regard to all the criteria used in this study. Second-order shallow water theory correctly predicts the mean net displacement. The Rayleigh and Boussinesq solu-

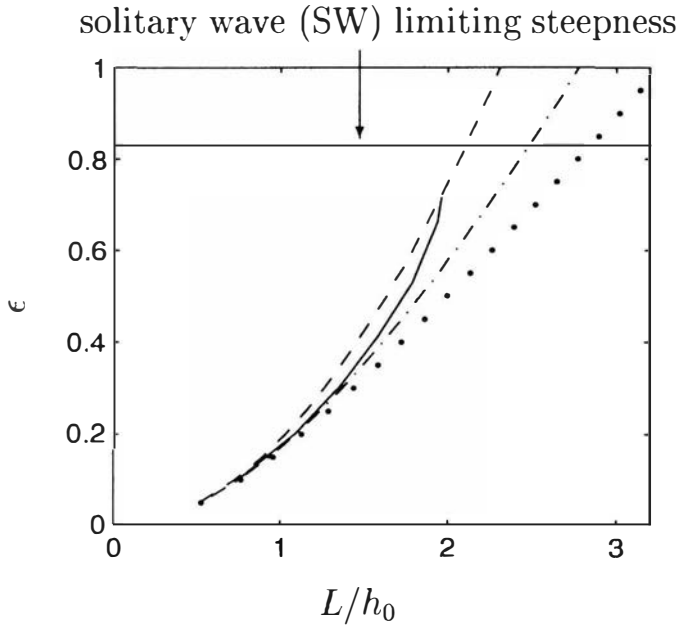

Fig. 12 Mean horizontal displacement obtained from Byatt-Smith's numerical solution (–), KdV (- -), second-order shallow water solutions (-.-) or Rayleigh's (...) analytical solutions versus solitary wave dimensionless amplitude ε ranging from 0 to 1.

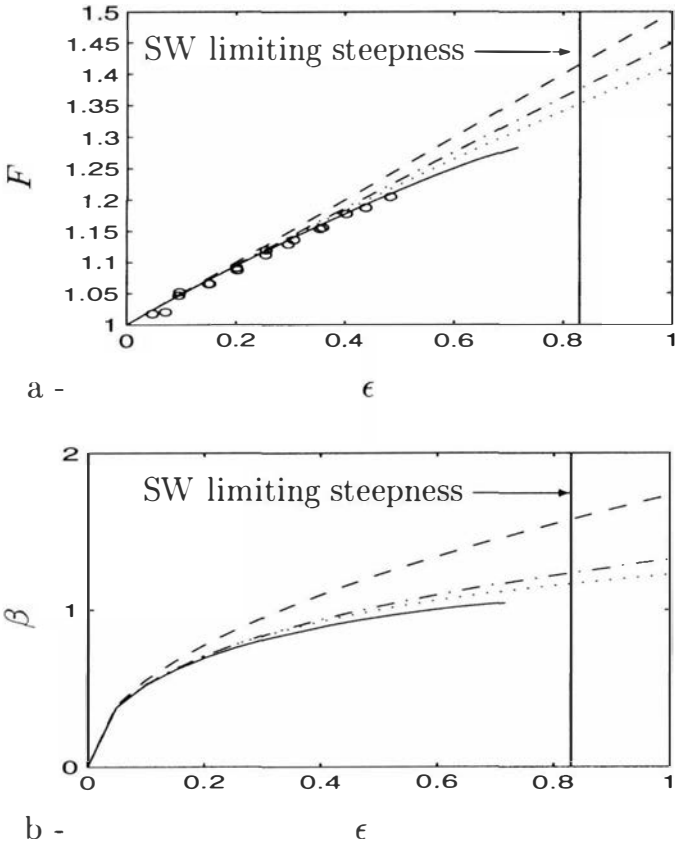

Fig. 14 Froude number versus solitary wave dimensionless amplitude (a) and outskirts decay coefficient versus Froude number (b) obtained for Byatt-Smith's numerical solution (–), KdV (- -), second-order shallow water theory (-.-) or Rayleigh's (...) analytical solutions and experiments (o).

tions agree with Byatt-Smith's numerical solution concerning the maximum velocity at mid-stroke. And finally paddle velocity derived from Byatt-Smith's numerical solution is matched by Rayleigh-based paddle velocity at the outskirts.

We can now understand why, by increasing the duration of motion for a given stroke, Goring reduces the waves trailing the first solitary wave. Indeed, the duration of motion as expressed by (7) is a function of both the phase speed c and the outskirts decay coefficient β of the solitary wave. To a given stroke corresponds a given outskirts decay coefficient. Thus, to prolong the duration of motion it would be necessary to take a smaller phase speed than the one corresponding to the outskirts decay coefficient in Boussinesq form. This is in agreement with the relation in Byatt-Smith's numerical solution between outskirts decay coefficient, phase speed and solitary wave amplitude. Thus, prolonging the duration of motion tends to match both outskirts decay coefficient and phase speed to the Byatt-Smith solution but for a smaller amplitude than the design one. As a consequence, the relation between the net displacement (paddle stroke) and solitary wave amplitude will tend to be fulfilled since in Boussinesq's solitary wave the net displacement was underestimated. But how much should we prolong motion duration to get the purest solitary waves? Goring suggested 10 % but this value actually depends on the solitary wave amplitude and hence is not constant. Therefore, we suggest using Rayleigh's procedure rather than Goring's because it is then unnecessary to modify the duration of paddle motion arbitrarily and the resulting solitary waves are as pure and more rapidly established.

6. Conclusion

It has been shown in this paper that solitary waves generated using a paddle law of motion derived from Rayleigh's solution (linearized or fitted) are purer and more rapidly established than with any of the shallow-water theory-based procedures. Trailing waves after solitary waves generated using this new procedure are indeed as small as in Goring's procedure, being less than 3 % of the main pulse amplitude. However, none of these generation procedures is perfect. Indeed, taking Byatt-Smith's (1970, [3]) numerical solution as a reference for the solitary wave solution, the paddle stroke is better described by second-order shallow-water theory than in the other procedures, whereas the maximum paddle velocity at mid-stroke is better predicted in our procedure or in Goring's. With respect to solitary wave generation, we suggest that this maximum paddle velocity is a key parameter. For a given maximum velocity, a Froude number is selected. The corresponding paddle stroke for this Froude number should then be prescribed. We found that the Rayleigh solitary wave with an accurate description of the Froude number and outskirts decay coefficient meet the above requirements. Hence the generation procedures based on Rayleigh's solitary wave solution is a good compromise for obtaining quite pure and rapidly established solitary waves.

7. Acknowledgements

The authors would like to thank Jean-Marc Barnoud for technical support and assistance when performing the experiments. This work has been financially supported by the MAST-III EC programme, under contract MAS3-CT95-0027. The first author is grateful to the French Ministry of Education for attributing her a PhD grant.

8. Notation

The following notations are used in the paper:

A	solitary wave main pulse amplitude
a'	first trailing wave amplitude
A'	second-order solitary wave amplitude
c	solitary wave phase speed
$F = c/\sqrt{gh_0}$	Froude number
g	gravity
h_0	mean water depth
L	solitary wave depth averaged mass displacement
S	paddle stroke
$Ur = \varepsilon/\sigma_2$	Ursell number
$u(x,t)$	depth-averaged horizontal velocity of solitary wave
t	time
X	Lagrangian space variable giving paddle position
x	space position in flume

α	tanh fit parameter
β	solitary wave outskirts decay coefficient
δ	tanh fit parameter
$\varepsilon = A/h_0$	dimensionless solitary amplitude
$\wedge = 2/\beta$	horizontal solitary wave length scale
$\gamma(x,t)$	vertical acceleration at free surface
$\eta(x,t)$	free surface elevation
$\theta = ct - X$	solitary wave co-moving frame variable
$\sigma = h_0/\wedge$	shallow water parameter
τ	duration of paddle motion

The following subscripts are used in the paper:

B	Boussinesq solitary wave expression
G	Goring generation procedure
KdV	Korteweg and De Vries solitary wave solution
R	Rayleigh solitary wave solution
SW2	second-order shallow water theory
t	derivation with respect to time
x	derivation with respect to space

9. References

[1] BOUSSINESQ M.J., Théorie de l'intumescence liquide, appelée onde solitaire ou de translation, se propageant dans un canal rectangulaire, C.-R. Acad. Sci. Paris, 72(1871), p 755-59.

[2] BOUSSINESQ M.J., Théorie des ondes et des remous qui se propagent le long d'un canal rectangulaire horizontal, en communiquant au liquide contenu dans un canal des vitesses sensiblement pareilles de la surface au fond, J. Math. Pure et Appl., 2(17)(1872), p 55-108.

[3] BYATT-SMITH J.G.B., An exact integral equation for steady surface waves, Proc. Roy. Soc. London, A. 315(1970), p 405-418.

[4] BYATT-SMITH J.G.B. and Longuet-Higgins M.S., On the speed and profile of steep solitary waves, Proc. Roy. Soc. London, A. 350(1976), p 175-189.

[5] CLAMOND D. and GERMAIN J.-P., Interaction between a Stokes wave packet and a solitary wave, Eur. J. Mech. B/Fluids, 18(1)(1999), p 67-91.

[6] DAILY J.W. and STEPHAN S.C., The solitary wave: its celerity, internal velocity and amplitude attenuation in a horizontal smooth channel, Proc. 3rd Conf. Coastal Eng., (1952), p 13-30.

[7] GORING D.G., Tsunamis – The propagation of long waves onto a shelf, PhD thesis of the California Institute of Technology, Pasadena, California (1978).

[8] GUIZIEN K., Les ondes longues internes: génération et interaction avec la houle, Thèse de l'Université Joseph Fourier, Grenoble (1998).

[9] GUIZIEN K. and BARTHÉLEMY E., Short waves modulations by large free surface solitary waves. Experiments and models., Phys. Fluids, 13(12), p 3624-3635.

[10] HAMMACK J.L. and SEGUR, H., The Korteweg-de Vries equation and water waves. Part 2. Comparison with experiments., J. Fluid Mech., 65(1974), p 289-314.

[11] KEULEGAN G.H., Gradual damping of solitary waves, J. Res. Nat. Bur. Standards, 40(1948), p 487-498.

[12] KORTEWEG D.J. and DE VRIES G., On the change of form of long waves advancing in a rectangular canal, and on a new type of stationary waves, Phil. Mag., 39(5)(1895), p 422-443.

[13] LAMB H., Hydrodynamics, Cambridge University Press, 6th ed. (1932), 738 p.

[14] LONGUET-HIGGINS M.S., Trajectories of particles at the surface of steep solitary waves, J. Fluid Mech., 110(1981), p 239-247.

[15] LONGUET-HIGGINS M.S. and FENTON J.D., On the mass, momentum, energy and circulation of a solitary wave. Part II., Proc. Roy. Soc., A 340(1974), p 471-493.

[16] MEI C.C., The applied dynamics of ocean surface waves, Advanced Series on Ocean Engineering, (1992), World Scientific.

[17] MILES J.W., Solitary waves., Ann. Rev. Fluid Mech., 12(1980), p 11-43.

[18] RAYLEIGH LORD, On waves., Phil. Mag., 1(1876), p 257-279.

[19] RENOUARD D.P., Seabra-Santos F.J. and Temperville A.M., Experimental study of the generation, damping, and reflection of a solitary wave, Dynamics of Atm. and Oceans, 9(1985), p 341-358.

[20] RUSSEL J.S., Report on waves, Proc. 14th Meeting, Brit. Ass. Adv. Sci., York (1845), p 311-390.

[21] SERRE F., Contribution à l'étude des écoulements permanents et variables dans les canaux, La Houille Blanche, 8(1953), p 374-388.

[22] SU C.H. and GARDNER C.S., KdV equation and generalisations. Part III. Derivation of Korteweg-de Vries equation and Burgers equation., J. of Math. Phys., 10(3)(1969), p 536-539.

[23] SYNOLAKIS C.E., Generation of long waves in laboratory, J. of Waterway, Port, Coastal, and Ocean Engineering, 116(2)(1990), p 252-266.

[24] TEMPERVILLE A., Contribution à l'étude des ondes de gravité en eau peu profonde, Thèse d'Etat, Université Joseph Fourier – Grenoble I (1985).

[25] WHITHAM G.B., Linear and non linear waves, Pure and Applied Mathematics Series, Ed. Wiley-Interscience, (1974).